Optical Monitoring of Polyesters Injection Molding

Alessandra Lucas Marinelli, Marcelo Farah, Rosario Elida Suman Bretas

Department of Materials Engineering, Universidade Federal de São Carlos, Rod. Washington Luiz, km 235, 13565–905 São Carlos, SP, Brazil

Received 12 August 2003; accepted 31 March 2005
DOI 10.1002/app.22491
Published online in Wiley InterScience (www.interscience.wiley.com).

ABSTRACT: An optical fiber sensor similar to the one developed by Thomas and Bur[1] was constructed for the monitoring of the crystallization of three polyesters during the injection molding process. The polyesters studied were: polybutylene terephthalate (PBT), polytrimethylene terephthalate (PTT), and polyethylene terephthalate (PET). With this optical system it was possible to obtain, in real time, some essential parameters of the polyester crystallization kinetics at different processing conditions. Thus, a study of the influence of injection molding variables on the nonisothermal crystallization kinetics of these polyesters was done. The processing variables were: mold wall and injection temperatures, T_w and T_i, respectively; flow rate, Q; and holding pressure, P_h. The experiments were done following a first order central composite design statistical analysis. The morphology of the samples was analyzed by polarized light optical microscopy, PLOM. The signal of the laser beam during the filling and the crystallization stages of the injection molding of these materials was found to be reproducible. The measurements showed that this system was sensitive to variations of the crystallization of different types of polymers under different processing conditions. The system was not able, however, to monitor the crystallization process when the crystallinity degree developed by the sample was very low, as in the PET resin. It was also observed that T_w and T_i were the most influential variables on the crystallization kinetics of PBT and PTT. Due to its slower crystallization kinetics, PTT was found to be more sensitive to changes in these parameters than the PBT. © 2005 Wiley Periodicals, Inc. J Appl Polym Sci 99: 563–579, 2006

Key words: crystallization; injection molding; light scattering; morphology; polyesters

INTRODUCTION

The injection molding of polymers is one of the most widely employed processing techniques. Today, due to the technological advances in this process, it is possible to produce highly sophisticated parts with reduced cycles. It is known, however, that for an efficient process, the mold geometry should be optimized. On the other hand, the high cost of these molds makes further changes after their construction highly expensive. Thus, it is recommended to determine the optimum and balance mold geometry before the injection molding. This determination can be made by the use of simulation softwares like the Moldflow® and Moldex®. These softwares, however, still do not take into account the polymer crystallization during the cooling stage, which will strongly determine the time needed for cooling (and, hence, the entire cycle of the process) and the warpage and shrinkage of the article. To quantitatively describe the structure development during injection molding, data of the crystallization kinetics under processing conditions are required, which are difficult to obtain. For these reasons, there is a large interest in studying crystallization during injection molding.[2–4]

The characterization of the *in situ* crystallization of polymers during the injection molding process constitutes a challenging problem. Usually, this crystallization occurs under high gradients of temperature (during the whole process), pressure (essentially during the packing/holding stage), and high deformation (shear and elongational, essentially during the filling stage), which can produce different types of morphologies: amorphous and/or crystalline with quiescent and/or flow induced crystallization. The combination of all these factors governs the final properties along the injection molded sample.

A high amount of research has been done on the development of experimental devices that directly monitor the solidification process during injection molding; these devices are based on different techniques: dielectric spectroscopy,[5] ultrasound techniques,[6–7] and indentation tests,[8] among others. Thomas and Bur[1] constructed an optical sensor, which was mainly a detector of reflected light, that is, light that was transmitted through the resin, reflected on the opposite wall of the mold, and transmitted back through the resin to the optical sensor. Although the results shown by the authors were very promising, they did not explore the new tool to verify, exten-

Correspondence to: R. E. S. Bretas (bretas@power.ufscar.br).

TABLE I
Molecular Weights and Melting Temperatures of the Polyesters

Polyester	Mark–Houwink coefficient α	Mark–Houwink coefficient K (dl/g)	$[\eta]$ (dl/g)	M_n (g/mol)	M_w (g/mol)	T_m (°C)
PBT[a]	0.871	7.39×10^{-5}	1.24		7.48×10^4	225
PTT[b]	0.69	5.36×10^{-4}	0.94		5.03×10^4	229
PET[c]	0.64	1.40×10^{-3}	0.96	3.60×10^4		247

[a] From ref.[25]
[b] From ref.[23]
[c] From ref.[24]

sively, how the injection molding process conditions would affect crystallization during processing, for different materials.

Recently, an attempt to obtain real-time crystallization during fast cooling was carried out using depolarized light detection and light scattering techniques, proposed by Magill[9–12] in the 1960s, after being employed by Stein et al.[13,14] Ding and Spruiell[15] and Lamberti et al.[16] designed and built an experimental set able to carry out very fast cooling rates with simultaneous detection of overall and depolarized light intensities emerging from solidifying samples. The qualitative behavior of the optical signals reported by Lamberti et al.[16] agreed well with the Ding and Spruiell[15] results, both showing a minimum in the overall and depolarized emerging light intensities during crystallization.

Chrisman et al.[17] also developed a method for optically determining the onset of crystallization of dissolved solids from solvent or mother liquor. The method relies on reflection and backscattering of light for detection of crystallization.

In this article we will present results obtained from the optical monitoring of the injection molding of polyesters under different processing conditions, using an optical sensor similar to that developed by Thomas and Bur.[1]

EXPERIMENTAL

Materials

For calibration of the light intensity signal, polystyrene (PS), from BASF, and polypropylene (PP), from Braskem of Brazil, were used. The study of the crystallization was made with a PET, kindly donated by MG-Rhodia-Ster, Brazil; a PBT, kindly donated by GE Plastics–South America, Brazil; and a

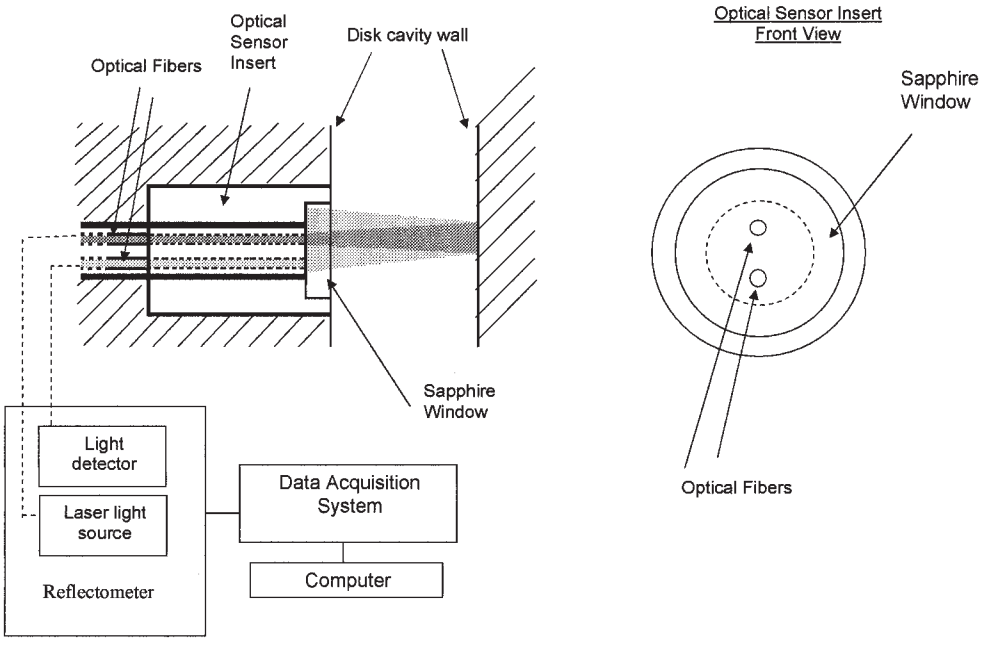

Figure 1 General scheme of the optical system.

TABLE II
Matrix of the First Order Central Composite Design of Experiments and Injection Conditions

N°	T_W (°C)	T_I (°C)	Q(cm^3/s)	P_h (bar)	Injection condition–PBT ($T_w/T_i/Q/P_h$)	Injection condition–PET ($T_w/T_i/Q/P_h$)	Injection condition–PTT ($T_w/T_i/Q/P_h$)
1	−1	−1	−1	−1	30/240/5/200	30/240/5/350	30/240/5/300
2	−1	−1	−1	−1	90/240/5/200	90/240/5/350	90/240/5/300
3	−1	1	−1	−1	30/260/5/200	30/260/5/350	30/260/5/300
4	1	1	−1	−1	90/260/5/200	90/260/5/350	90/260/5/300
5	−1	−1	1	−1	30/240/65/200	30/240/65/350	30/240/65/300
6	1	−1	1	−1	90/240/65/200	90/240/65/350	90/240/65/300
7	−1	1	1	−1	30/260/65/200	30/260/65/350	30/260/65/300
8	1	1	1	−1	90/260/65/200	90/260/65/350	90/260/65/300
9	−1	−1	−1	1	30/240/5/600	30/240/5/550	30/240/5/600
10	1	−1	−1	1	90/240/5/600	90/240/5/550	90/240/5/600
11	−1	1	−1	1	30/260/5/600	30/260/5/550	30/260/5/600
12	1	1	−1	1	90/260/5/600	90/260/5/550	90/260/5/600
13	−1	−1	1	1	30/240/65/600	30/240/65/550	30/240/65/600
14	1	−1	1	1	90/240/65/600	90/240/65/550	90/240/65/600
15	−1	1	1	1	30/260/65/600	30/260/65/550	30/260/65/600
16	1	1	1	1	90/260/65/600	90/260/65/550	90/260/65/600
17	0	0	0	0	60/250/35/400	60/250/35/450	60/250/35/450
18	0	0	0	0	60/250/35/400	60/250/35/450	60/250/35/450

PTT, kindly donated by Shell Chemicals, USA. The materials were dried for 5 h at 150°C in a vacuum chamber, to avoid hydrolytic degradation.

These polyesters were chosen because of their crystallization kinetics behavior, which is faster for PBT and much slower for PET, due to the lower amount of aliphatic carbons in the chain of PET. Also, the morphological characteristics of injection molded samples of these materials are much less explored in the literature, in comparison with polyolefins.

The molecular weights and the melting temperature of the three materials are shown in Table I. The weight and number average molecular weights, M_w and M_n, respectively, of the polyesters were measured by solution viscosity by Farah and Bretas.[18] A solution of phenol and 1,1,2,2–tetrachloroethane, 60/40(w/w), at 30°C for

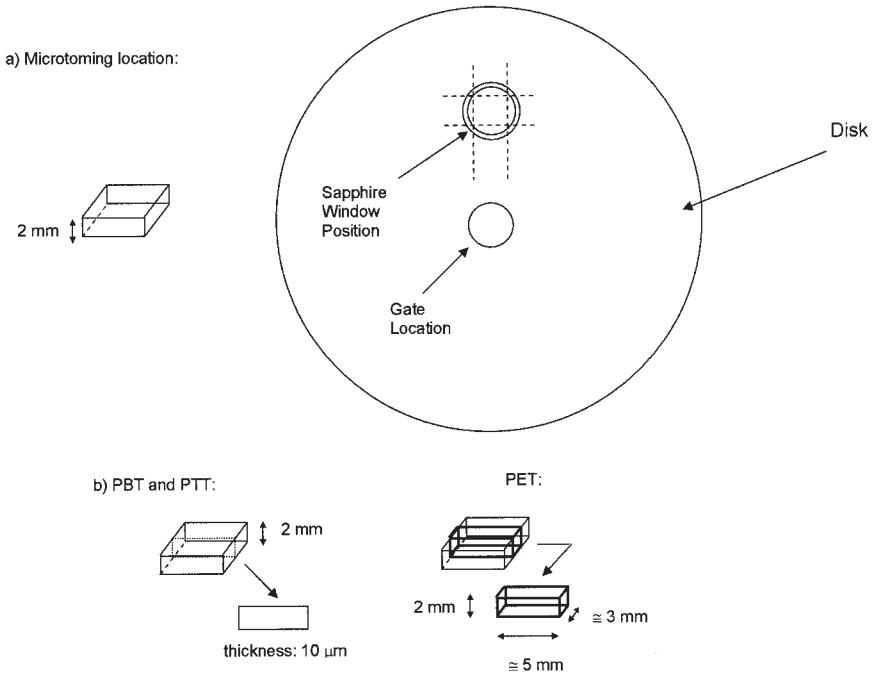

Figure 2 Samples for morphological characterization: (a) samples location in the disk; (b) samples cutting.

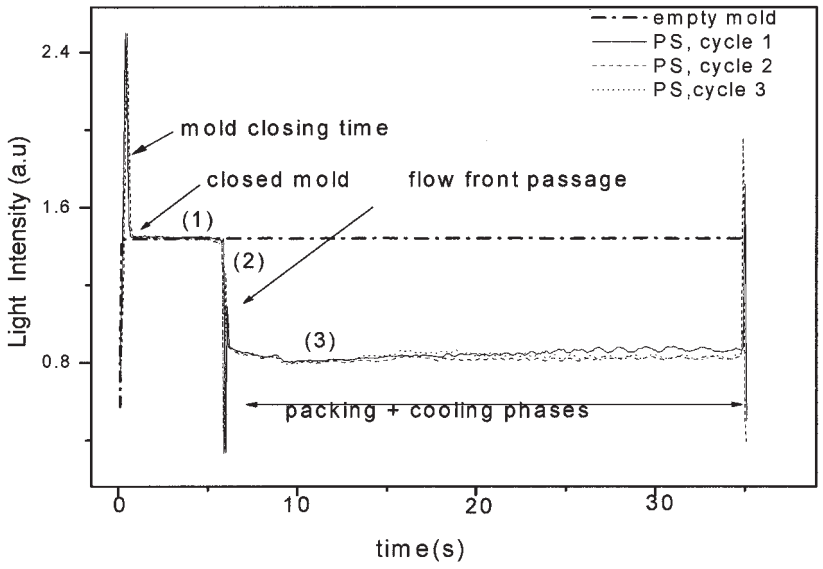

Figure 3 Light intensity signal as a function of cycle time for the empty mold and for the PS injection molding.

the PBT and PTT and at 25°C for the PET was used. To determine M_w or M_n, the Mark–Houwink[19] equation was used:

$$[\eta] = KM_v^{\alpha} \tag{1}$$

where K and α are constants depending on the polymer and solvent system, M_v = viscosimetric molecular weight, and $[\eta]$ is the intrinsic viscosity. The intrinsic viscosity was determined by the equation given by Rao and Yassen,[20] Chee,[21] and Chuah et al.,[22] as shown below:

$$[\eta] = \frac{(\eta_{sp} + \ln \eta_{rel})}{2c} \tag{2}$$

where η_{sp} is the specific viscosity given by

$$\eta_{sp} = \eta_{rel} - 1$$

η_{rel} is the relative viscosity given by $\eta_{rel} = \eta/\eta_0$, η is the measured viscosity, η_0 is the solvent viscosity, and c is the solution concentration. The Mark–Houwink coefficients[23,24] are also shown in Table I.

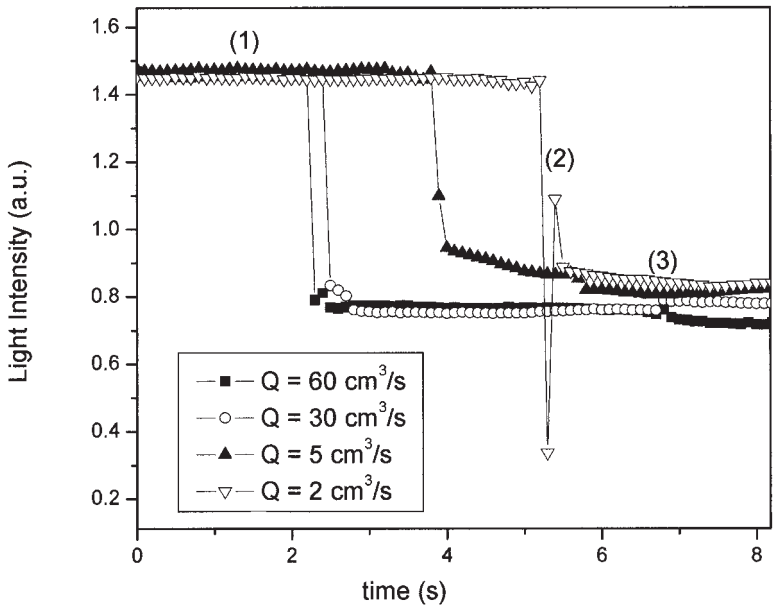

Figure 4 Light intensity signal for the PS injection molding at different flow rates.

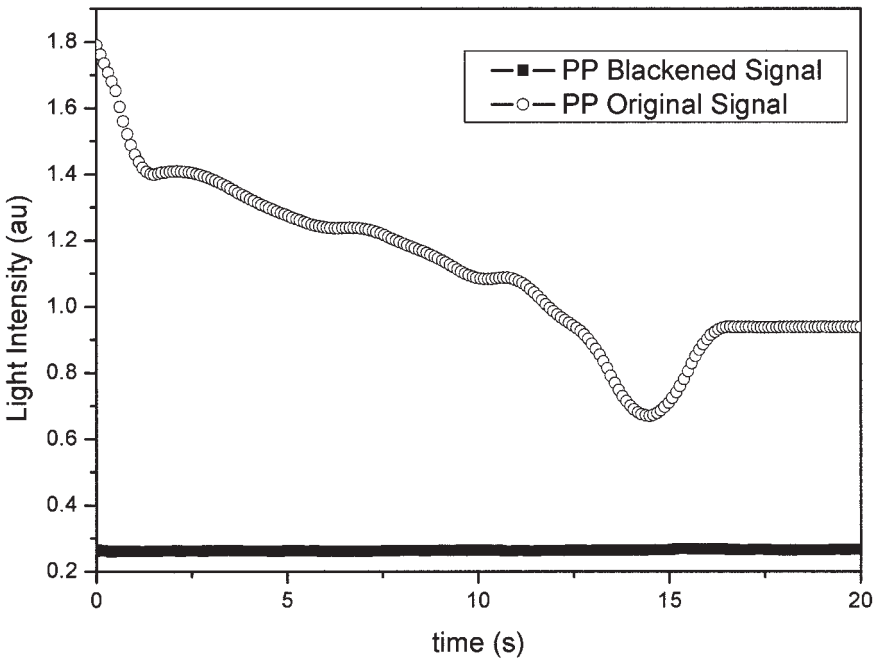

Figure 5 Light intensity signal for the PP injection molding.

The melting temperature, T_m, was measured by differential scanning calorimetry, DSC. The polyesters were heated at 10°C/min between 30 and 300°C, in a DSC 7, from Perkin–Elmer, under N_2 atmosphere.

Injection mold instrumentation with an optical sensor and a pressure transducer

The mold cavity was a disk (diameter d = 90 mm, thickness h = 2 mm, central injection location). The optical device was installed at 30 mm from the center of the disk. In the same position, but on the opposite side, a pressure transducer (Kistler, 6152A) was also installed, because simulation results done with the Moldflow® software indicated similarity of the flow and cooling conditions at these two points.

The optical device consisted of two 600 μm diameter optical fiber cables: one connected to a laser light source and the other one to a laser light detector. An AITA-MARTIN Optical Reflectometer was used, with a 15 mW HeNe laser light source, of 632.8 nm wavelength and a detector (photodiode). To avoid damage to the optical cables, a sapphire window was installed flush with the mold wall. Figure 1 shows a general

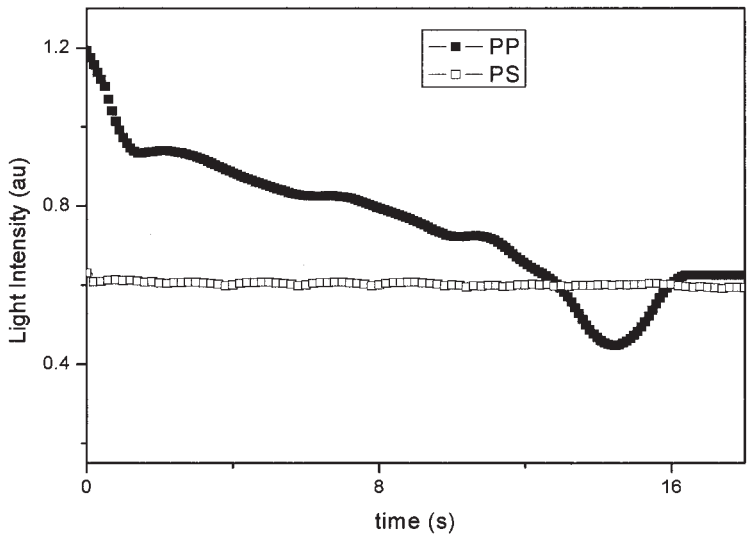

Figure 6 Comparison between the PP and PS light intensity signals injected at the same flow rate.

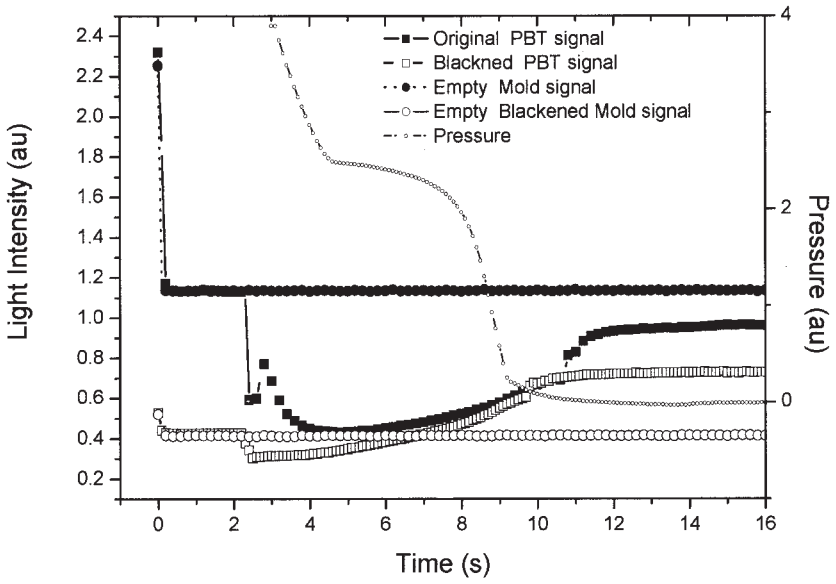

Figure 7 Standard light intensity signals of the PBT injection molding.

scheme of the system with details of the disk cavity insert. Data acquisition was made through the use of a Semp–Toshiba computer interfaced with the mold, using an acquisition data card from National Instruments, NI-DAQ, which was plugged together with a shielded carrier model SC-2345 with the signal condition modules SC-TC02, SC-AI04, and SC-AI03.

To test a surface that completely would absorb the incident light, the opposite cavity wall was covered with a black tape. To test a surface that would reflect the total incident light, the mold was tested empty.

Like the optical device developed by Thomas and Bur,[1] the measured optical signal was the result of the intensity of the light transmitted through the resin, reflected on the opposite cavity wall, and transmitted back through the resin to the optical sensor, that is, light transmitted twice through the resin. Besides light absorption, the polymer can also scatter light; scattering (and backscattering) occurs when the polymer particle has a size equal to or higher than the light wavelength. Besides this influence, backscattering also depends on the crystal density (closely packed crystals are known to backscatter more). In our case, the light wavelength was 632.8 nm. A unit cell has a typical size between 0.2 and 2 nm, and a lamellae crystal thickness between 5 and 50 nm, while spherulites have sizes

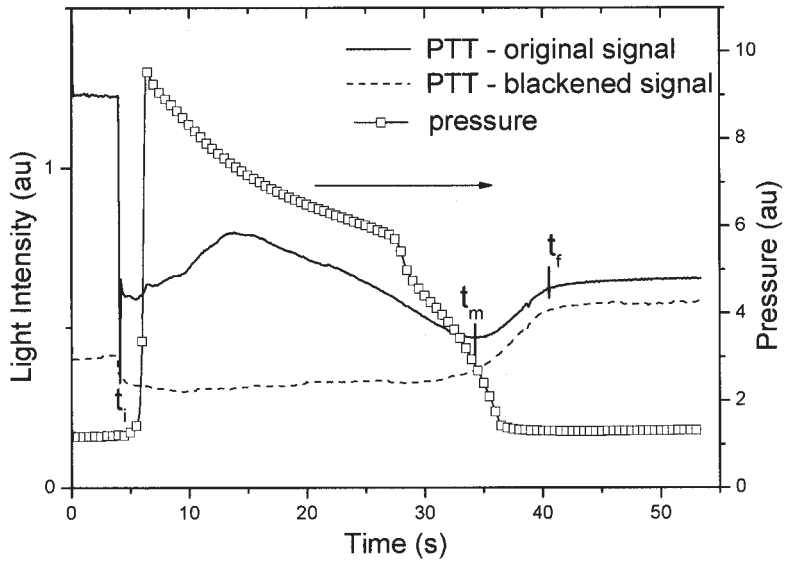

Figure 8 Standard light intensity signals of the PTT injection molding.

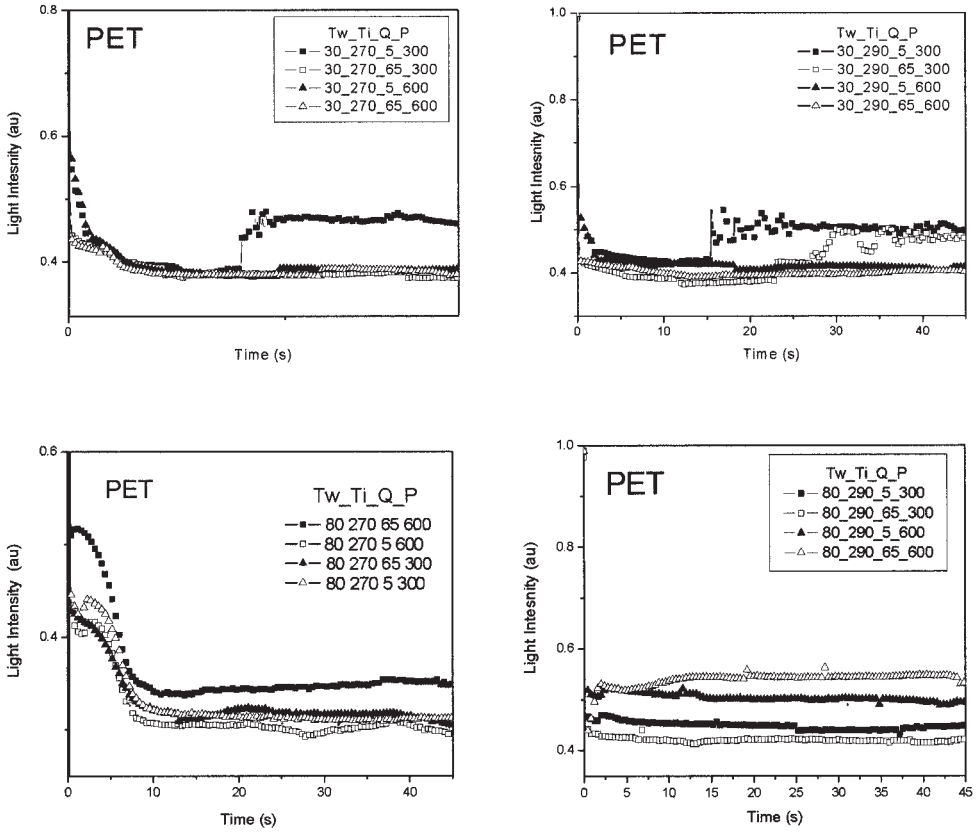

Figure 9 Light intensity signals of the PET injection molding at different molding conditions.

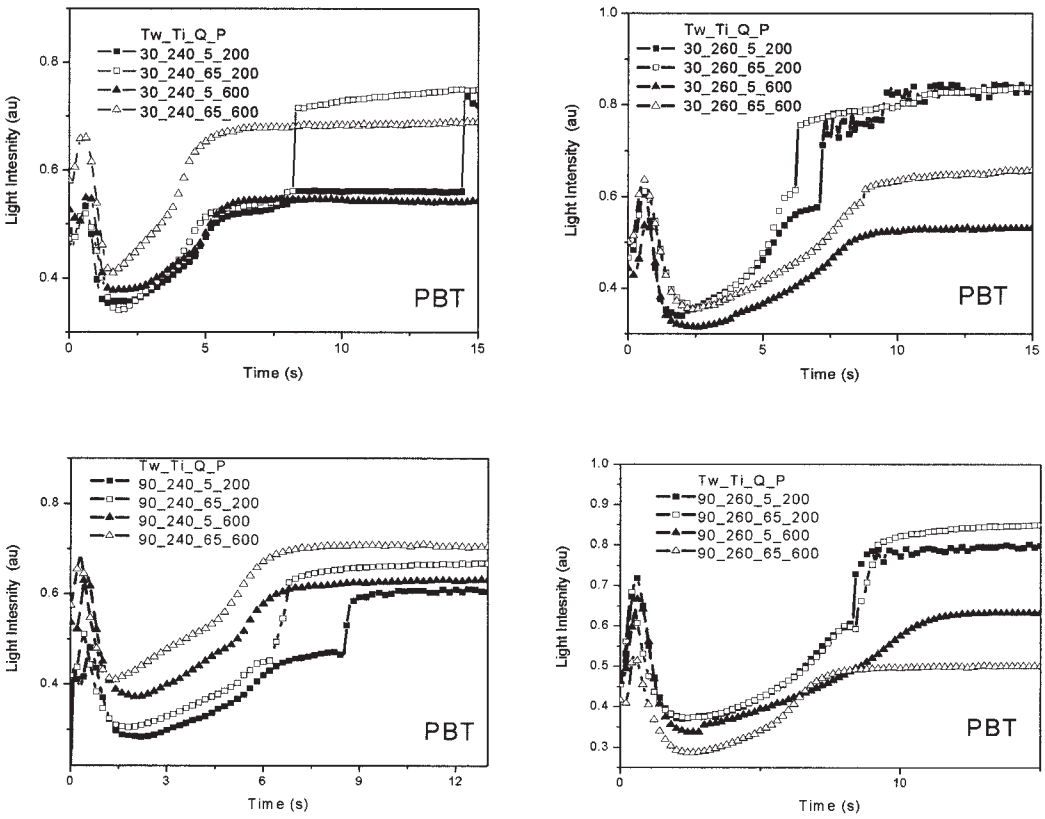

Figure 10 Light intensity signals of the PBT injection molding at different molding conditions.

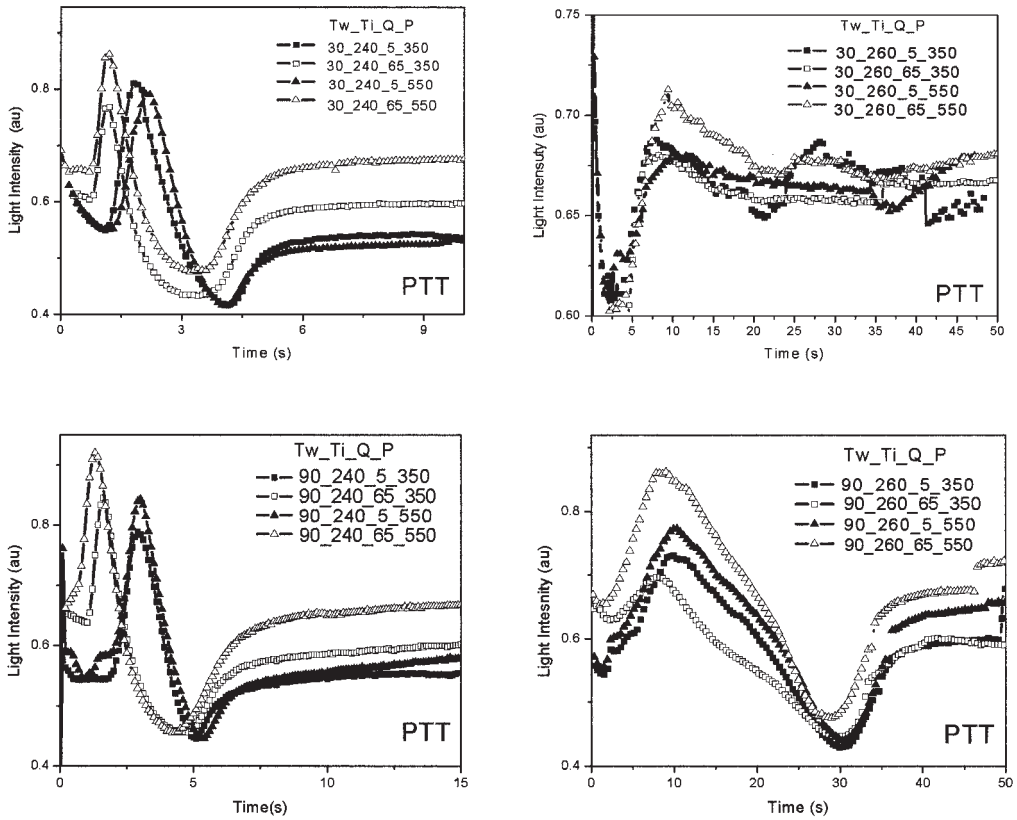

Figure 11 Light intensity signals of the PTT injection molding at different molding conditions.

between 1 and 100 μm. Therefore, we will expect that the optical fiber sensor will detect scattering and back-scattering from structures larger than the lamellar crystal thickness.

TABLE III
Crystallization Characteristic Times Obtained from the Analysis of the PBT Curves

Molding condition ($T_w/T_i/Q/P_h$)	t_m (s)	t_f (s)
30/240/5/200	1.6	6.6
30/240/5/600	1.6	7.3
30/240/65/200	1.7	6.0
30/240/65/600	1.6	9.2
90/240/5/200	2.1	9.7
90/240/5/600	2.0	10.1
90/240/65/200	1.8	11.2
90/240/65/600	1.3	8.0
30/260/5/200	2.0	7.1
30/260/5/600	2.6	9
30/260/65/200	2.2	7.1
30/260/65/600	2.6	9.2
90/260/5/200	2.1	11.5
90/260/5/600	2.4	11.8
90/260/65/200	2.3	10.8
90/260/65/600	2.5	13.2
60/250/35/400	2.0	12

Injection molding

The injection molding of the disks was made in an injection molding machine ARBURG 270V, with a clamping force of 80 tons and screw diameter of 30 mm. A heating/cooling mold unity HB W 140, from HB THERM, was used to control the mold temperature. An iron-constantan thermocouple was used to check the mold temperature periodically. To evaluate

TABLE IV
Crystallization Characteristic Times Obtained from the Analysis of the PTT Curves

Molding condition ($T_w/T_i/Q/P_h$)	t_m (s)	t_f (s)
30/240/5/350	4.3	10.3
30/240/5/550	4.1	8.6
30/240/65/350	2.9	6.3
30/240/65/550	3.7	6.5
90/240/5/350	5.1	13.6
90/240/5/550	4.9	15
90/240/65/350	5.5	8.4
90/240/65/550	4.0	8.5
90/260/5/350	30.1	42.7
90/260/5/550	30.3	43.6
90/260/65/350	29.7	40.7
90/260/65/550	28.5	39.8
60/250/35/450	14.9	19.7

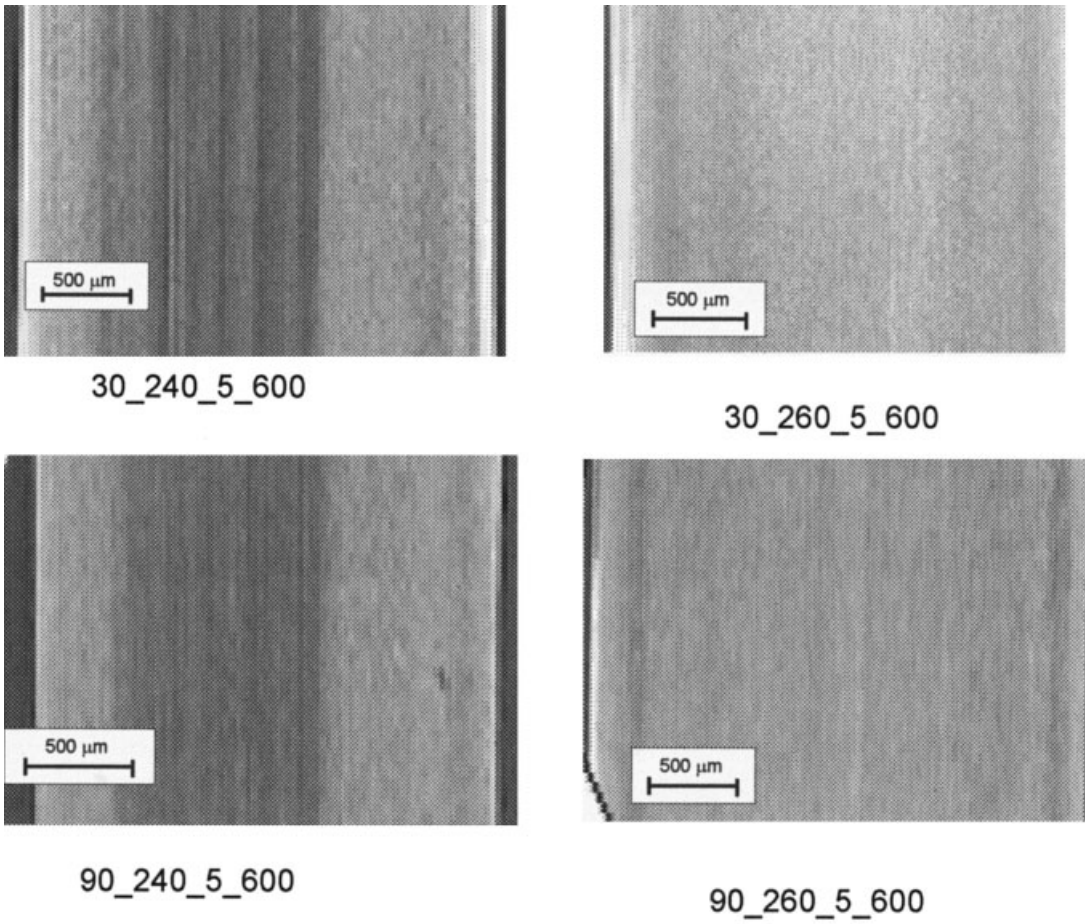

Figure 12 Standard morphologies of the PBT samples at different molding conditions.

the influence of the injection molding conditions on the crystallization of the polyesters, four conditions were varied: mold wall temperature, T_w; injection temperature, T_i; injection flow rate, Q; and holding pressure, P_h. From the literature[25] it is known that these variables have the highest influence on the shrinkage of injection molding articles. Because the shrinkage is a direct function of the crystallization of semi crystalline polymers, these variables were chosen to study the crystallization kinetics during the injection molding.

The processing window of the polyesters was determined after finding a compromise between the material, the injection molding machine, and the disk mold geometry limits, guaranteeing useful injected articles and reliable optical sensor signals. The limits of T_w were chosen between 30 and 90°C because water was the cooling medium. The lower T_i, for each polyester, was chosen to be about 10°C higher than its melting temperature, while the higher T_i was chosen to avoid thermal degradation of the polyester. The lower Q, 5 cm^3/s, corresponded to the minimum flow rate in which the cavity was fulfilled, while the higher limit, 65 cm^3/s, corresponded to the machine limit. The lower P_h limit for each polyester was determined as the minimum holding pressure that would guarantee no superficial defects. The highest P_h was chosen based on the clamp force of the machine, which means that that value would not allow the opening of the mold during the filling and holding stages.

Statistical analysis

To identify the most influential factors and the interactions between these factors, a variance analysis, ANOVA, was used, which shares the total variations resulting from the main factors, from the interactions between these factors, and from the error.

A central composite design was used to construct response surfaces. It consisted of a two level planning (2k, where k is the number of factors or independent variables), codified as −1 and +1, augmented by a central point, and used to test the surface curvature.

Once the experimental limits of the variables were set, the first order central composite design of the experiments (cube portion only) was set, which gave 18 experimental conditions. Table II shows the resultant planning matrix. In this table, levels −1, 0, and +1

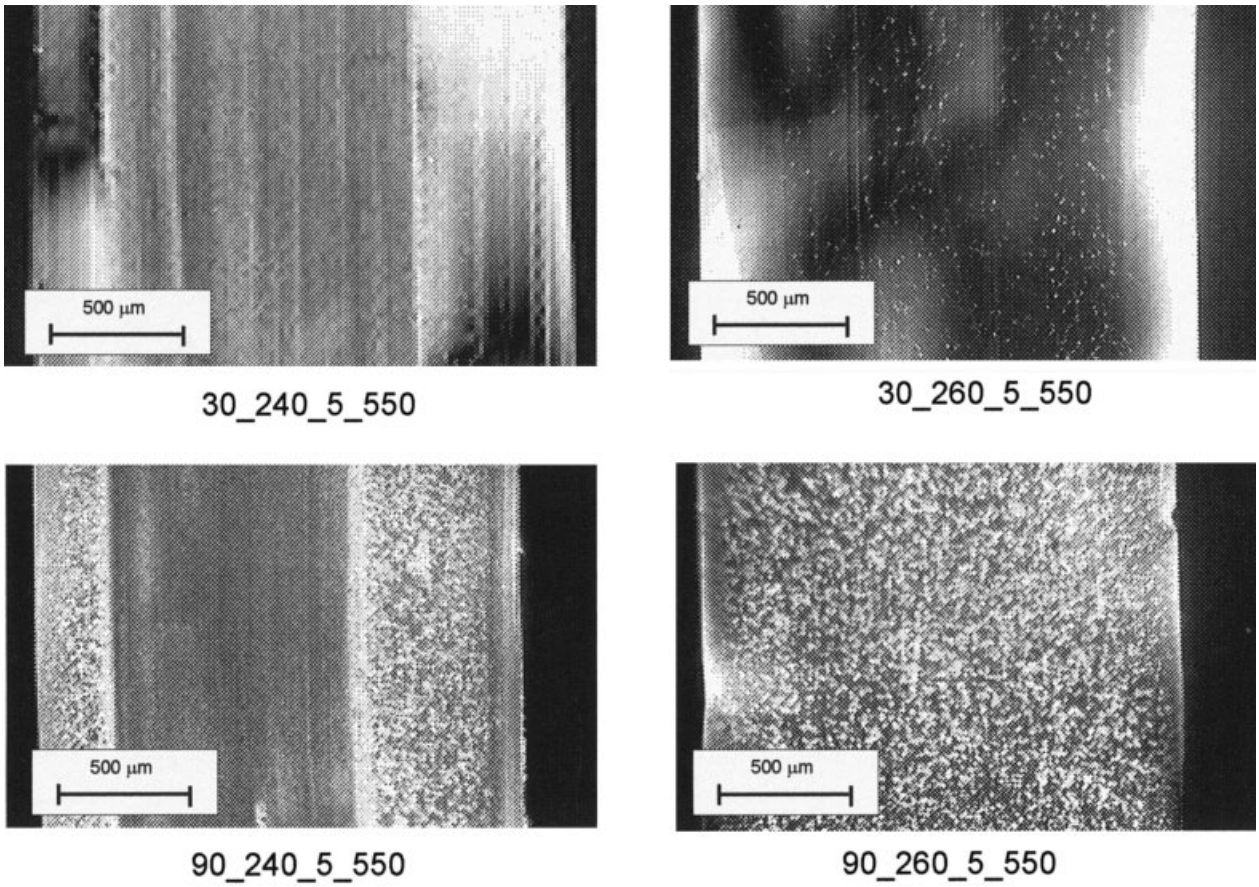

Figure 13 Standard morphologies of the PTT samples at different molding conditions.

represent the inferior, the central, and the superior levels of the variables, respectively.

The quadratic components of the relationships between the factors and the dependent variables were expressed by a second order degree polynomial as:

$$y = b_0 + \Sigma b_i x_j + \Sigma b_i x_j^2 + \Sigma\Sigma b_{ij} x_i x_j \qquad (3)$$

where:

$x_1, \ldots, x_i$ are the main effects;
$x_1 x_2, x_1 x_3, \ldots, x_{i-1} x_i$ are the two-factor interactions;
$(x_1^2, \ldots, x_i^2)$ are the quadratic terms; and
b_i are the coefficients of the polynomial.

These coefficients are unknown, but can be estimated from a regression analysis based on the least-square method.[26–28] To identify the most influential factors and the interactions between these factors an Analysis of Variance, ANOVA, was done using the software STATISTICA® (v.4.3). The value of the *p*-level represents a decreasing index of the result reliability. The higher the *p*-level, the less we can believe that the observed relation between variables in the sample is a reliable indicator of the relation between the respective variables in the population. The *p*-level of 0.05 is customarily treated as a "borderline acceptable" error level, but depending on the process, it can be changed to smaller or higher values.

The model fitting was quantified by the ratio $R^2 = SQ_R/SQ_T$, where SQ_R and SQ_T were the quadratic sums due to regression and around the average, respectively. The more R^2 tends to 1, the more the variation around the average can be explained by the regression model.[26]

Morphological characterization

The injection-molded samples were microtomed in the region of the sapphire window, as sketched in Figure 2(a). A microtome HM360, from MICROM, was used. For the PBT and PTT samples, slices of 10 μm embedded in silicon oil were obtained and put between glass slides. For the PET samples, polished rectangular blocks were obtained, as sketched in Figure 2(b).

These samples were analyzed in a polarized light optical microscopy DMRXP, from Leica, coupled to a video camera and a PC, using the software Image Pro® Plus. For the PBT and PTT samples, polarized light was used. For the PET ones, the best result was obtained using no polarized light.

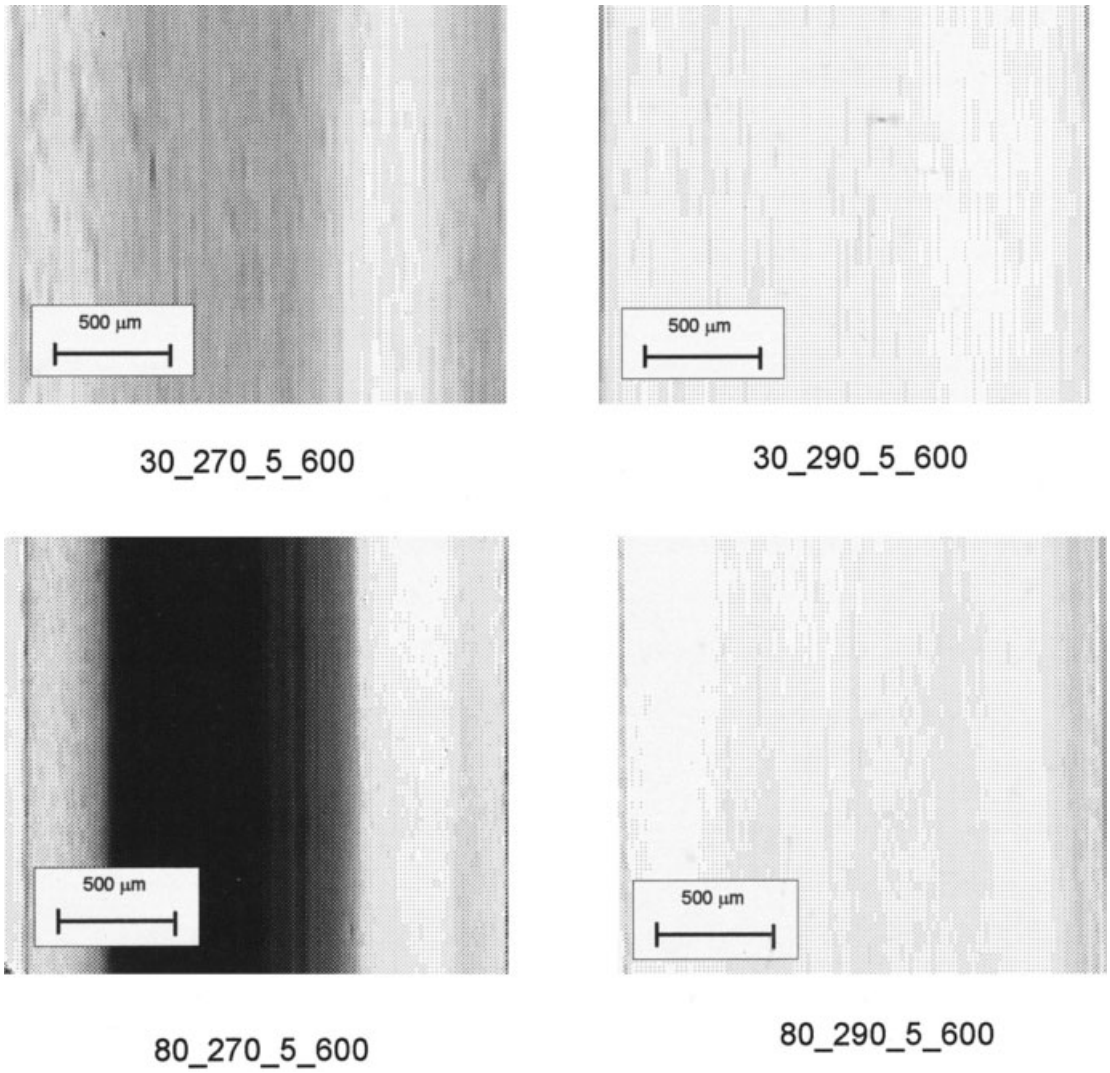

Figure 14 Standard morphologies of the PET samples at different molding conditions.

Differential scanning calorimetry (DSC)

To evaluate the overall crystallinity degree of the samples, X_c, a calorimeter from TA Instruments, model Q100, was used. X_c was calculated from eq. (4), after heating the sample at 40°C/min (to avoid recrystallization), under N_2 atmosphere:

$$Xc = \frac{\Delta H_m - \Delta H_c}{\Delta H_m^0} \times 100, \quad (4)$$

where:

ΔH_m = melting enthalpy;

ΔH_c = cold crystallization enthalpy;

ΔH_m^0 = melting equilibrium enthalpy;

(ΔH_m^0, PBT = 142 J/g[29]

ΔH_m^0, PTT = 144 J/g[30],andΔH_m^0, PET=145 J/g[31]).

RESULTS AND DISCUSSION

The first test done with the injection molding optical system was to evaluate the sensitivity and reproducibility of the optical sensor. Thus, the signal of the light intensity as a function of the cycle time, through an empty mold, was first monitored. Figure 3 shows the resultant signal curve. It can be observed that the signal increases abruptly up to a determined light intensity value (in this case, around 1.45 a.u) and remains with this value up to the end of the cycle. This intensity represents the intensity of the light that was reflected from the opposite mold wall. Because the mold was empty, there was no further variation of the light intensity signal as a function of time after the mold was closed.

TABLE V
Overall Crystallinity Degree, X_c, Evaluated by DSC

PBT samples	X_c (%)	PTT samples	X_c (%)	PET samples	X_c (%)
30/240/5/200	27.7	30/240/5/350	25.4	30/270/5/300	7.4
30/240/5/600	30.6	30/240/5/550	35.1	30/270/5/600	5.6
30/240/65/200	30.4	30/240/65/350	37.3	30/270/65/300	8.0
30/240/65/600	30.2	30/240/65/550	36.9	30/270/65/600	8.6
30/260/5/200	31.2	30/260/5/350	11.6	30/290/5/300	9.6
30/260/5/600	32.3	30/260/5/550	14.7	30/290/5/600	8.1
30/260/65/200	34.2	30/260/65/350	19.0	30/290/65/300	4.6
30/260/65/600	31.4	30/260/65/550	18.6	30/290/65/600	7.0
90/240/5/200	27.9	90/240/5/350	38.9	80/270/5/300	8.0
90/240/5/600	30.8	90/240/5/550	41.5	80/270/5/600	11.9
90/240/65/200	30.1	90/240/65/350	41.7	80/270/65/300	11.3
90/240/65/600	29.6	90/240/65/550	35.2	80/270/65/600	11.8
90/260/5/200	33.3	90/260/5/350	46.9	80/290/5/300	7.6
90/260/5/600	29.3	90/260/5/550	41.5	80/290/5/600	7.6
90/260/65/200	31.6	90/260/65/350	45.4	80/290/65/300	7.7
90/260/65/600	32.2	90/260/65/550	44.8	80/290/65/600	4.1
60/250/35/400	32.3	60/250/35/450	16.9	55/280/35/450	8.8

The next step was to evaluate the sensitivity of the optical detector to the passage of the flow front of an amorphous material. Thus, PS was injected in the mold cavity; the resultant light intensity curves are also shown in Figure 3. After the mold closes, a plateau appears (stage 1) similar to that obtained with the empty mold; when the polymer flow front passes along the sapphire window, the signal abruptly decreases (stage 2), then it has a small and abrupt increase, and after that, it remains almost constant during the whole packing/cooling stages (stage 3). The abrupt decrease (stage 2) occurs due to the mold filling, when the light will pass through a more dense and opaque material (the polymer melt) than air. Three consecutive cycles are shown in Figure 3, showing the excellent signal reproducibility of the optical system.

Figure 4 shows, in detail, the obtained signals at the moment of the passage of the flow front of the PS injected at different flow rates. It can be observed that the system is highly sensitive to the change in flow rates. The larger the flow rate, the smaller the time for the front flow to pass (the smaller the stage 1) and the lower the abrupt signal increase after stage 2.

Once the responses of the optical sensor to an empty mold and to the passage of the flow front of an amorphous material were known, a further step was to inject a semicrystalline material. Thus, PP was injected with this purpose. Figure 5 shows these results. The blackened signal also shown in Figure 5 corresponds to the mold, filled with PP, but having its opposite wall blackened. As said before, the light intensity signal is a summation of: (i) light transmitted through the resin with its intensity being attenuated by scattering and absorption, (ii) light reflected on the opposite wall, and (iii) light transmitted back through the resin with its intensity being decreased by the scattering and absorption and being increased by the backscattering. As observed, the PP crystallization does not have light backscattering, only absorption, confirming other works.[1,32] Also, it can be observed that there was a continuous decrease of the light intensity during the whole PP crystallization, as expected.

Figure 6 shows the signals obtained with PS and PP injected at the same flow rate. The time when the flow front reached the optical sensor was taken as t = 0 s. It can be observed that the light intensity curves of the two materials are quite different. It must be pointed out that optimum initial laser intensity for each kind of material should be found. For PP, for example, the best light intensity is much smaller than for the polyesters, due to its lower opacity.

Once the sensor ability to detect the crystallization process was determined, the injection molding of the polyesters was done. Figure 7 shows standard results

TABLE VI
Coefficients of the Polynomial (eq. (3)) for the PBT Samples

	b_0	T_w^2	T_w	T_I	Q	P
t_m	2.000	—	0.310	—	—	
t_f		−2.76[d]	1.55	0.73[e]	—	0.49[f]
	$T_w \cdot T_i$	$T_w \cdot Q$	$T_w \cdot P$	$T_i \cdot Q$	$T_i \cdot P$	R^2
t_m	—	−0.0625[b]	−0.0625[c]	0.087[a]	—	0.96
t_f	—	—	−0.5[g]	—		0.89

[a] $p = 0.06$.
[b] $p = 0.15$.
[c] $p = 0.15$.
[d] $p = 0.09$.
[e] $p = 0.07$.
[f] $p = 0.18$.
[g] $p = 0.17$.

TABLE VII
Coefficients of the Polynomial (eq. 3)) for the PTT Samples

	b_0	T_w^2	T_w	T_i	Q	$T_w \cdot Q$	$T_i \cdot Q$	R^2
t_m	14.9	1.8[b]	0.56[a]	12.387	−0.5[c]			0.999
t_f	19.7	5.11	1.73	15.16	−1.487	−0.7[d]	0.737[e]	0.999

[a] $p = 0.14$;
[b] $p = 0.13$;
[c] $p = 0.17$;
[d] $p = 0.19$;
[e] $p = 0.17$

obtained for a PBT injection molding cycle. This polymer has very fast crystallization kinetics. It can be observed that after the filling stage (at about 2.4 s), an abrupt signal increase occurs until approximately 2.7 s. After this increase, the light intensity decreases until 5s. After this value the signal again increases, until approximately 11.5 s. Finally, after 11.5 s, the light intensity signal remains constant. The cavity pressure curve is also shown in Figure 7. It can be observed that the pressure increases abruptly after the filling stage and attains its maximum at about 3.14 s (that is, in 0.71 s). Then, it decreases until approximately 11.5 s, attaining zero after this value.

In Figure 7, the light intensities when the mold is empty and when the opposite mold wall is blackened and the mold is filled with PBT and is empty are also shown. Comparing the blackened and filled with PBT curve and the original PBT curve, it can be concluded that, after 5 s, the light intensity signal of the PBT crystallization has a strong backscattering component, contrary to the PP behavior.

The difference between the empty and the empty blackened curves will give the intensity of the wall reflected and re-transmitted light, which it can be seen, will be very high.

Analyzing the standard original PBT signal shown in Figure 7, it can be concluded that the light intensity decrease in stage 2 is due to the mold filling and instantaneous formation of a wall frozen crystalline and oriented layer. The thickness of this layer is a function of the flow rate (the lower the flow rate, the larger the thickness). In any case, at that point the packing pressure has not yet been applied to the cavity. Thus, the polymer will slightly separate from the wall, allowing light reflection from the opposite mold wall; therefore, a slight light signal increase occurs. However, right after, the packing pressure is applied to the cavity. This packing pressure and the still flowing melt will push again the molded polymer against the mold walls and, thus, the signal will again decrease.

As said before, the beginning of the crystallization occurred right after the filling stage; thus, the decrease of the light intensity until 5 s can be credited to the light scattering and absorption promoted by the still very small crystals. The observed minimum of the light intensity between 5 and 6s can be attributed to the formation of a spherulitic morphology.[1,15,33] Between 6 s and 10.5 s, however, the crystals attain sizes high enough to promote intense backscattering and the light intensity signal increases (the original and the blackened with PBT curves are similar up to this point). It can also be observed that at 10.5 s, the cavity pressure is almost zero; therefore, the molded and solidified polymer will detach from the walls. Then the further increase of the original PBT curve between 10.5 and 11.5s can be credited to the contribution of the opposite wall reflected light and subsequent re-transmission. After 11.5 s, the cavity pressure is finally zero and, thus, the plateau after this value represents the contribution of all factors.

Similar results were found for the PTT. Figure 8 shows standard results. It can be observed that due to the PTT lower crystallization rate, the curves are shifted to higher times and are different from those of the PBT. After the filling stage (about 4 s, in this case), there is an instantaneous signal increase and then a decrease until approximately 6 s. At this point the packing pressure is applied and attains its maximum. From 6 s up to approximately 13.3 s, the signal increases again; between 13.3 and 35 s it decreases, increasing again between 35 and 40 s. After 40 s, a plateau is attained and the pressure cavity is zero.

Between 0 and 32 s, there was no backscattering contribution to the signal. The behavior between 4 s and 6 s can be explained as in the PBT case (opposite wall reflected light). On the other hand, the observed signal increase between 6 and 13.3 s can be credited to the strong reflected and re-transmitted light contributions (little light scattering and absorption). This means that the crystalline entities in this time interval were smaller than the light wavelength. Between 13.3 s and 32 s, the formation of the spherulitic morphology occurred and the light signal decreased due to the light scattering; however, the crystal sizes were still small and no backscatter occurred. Between 32 s and 35 s, backscattering contributed, but the light scattering contribution was still higher. After 35 s, the backscattering contribution is the strongest and the signal increased.

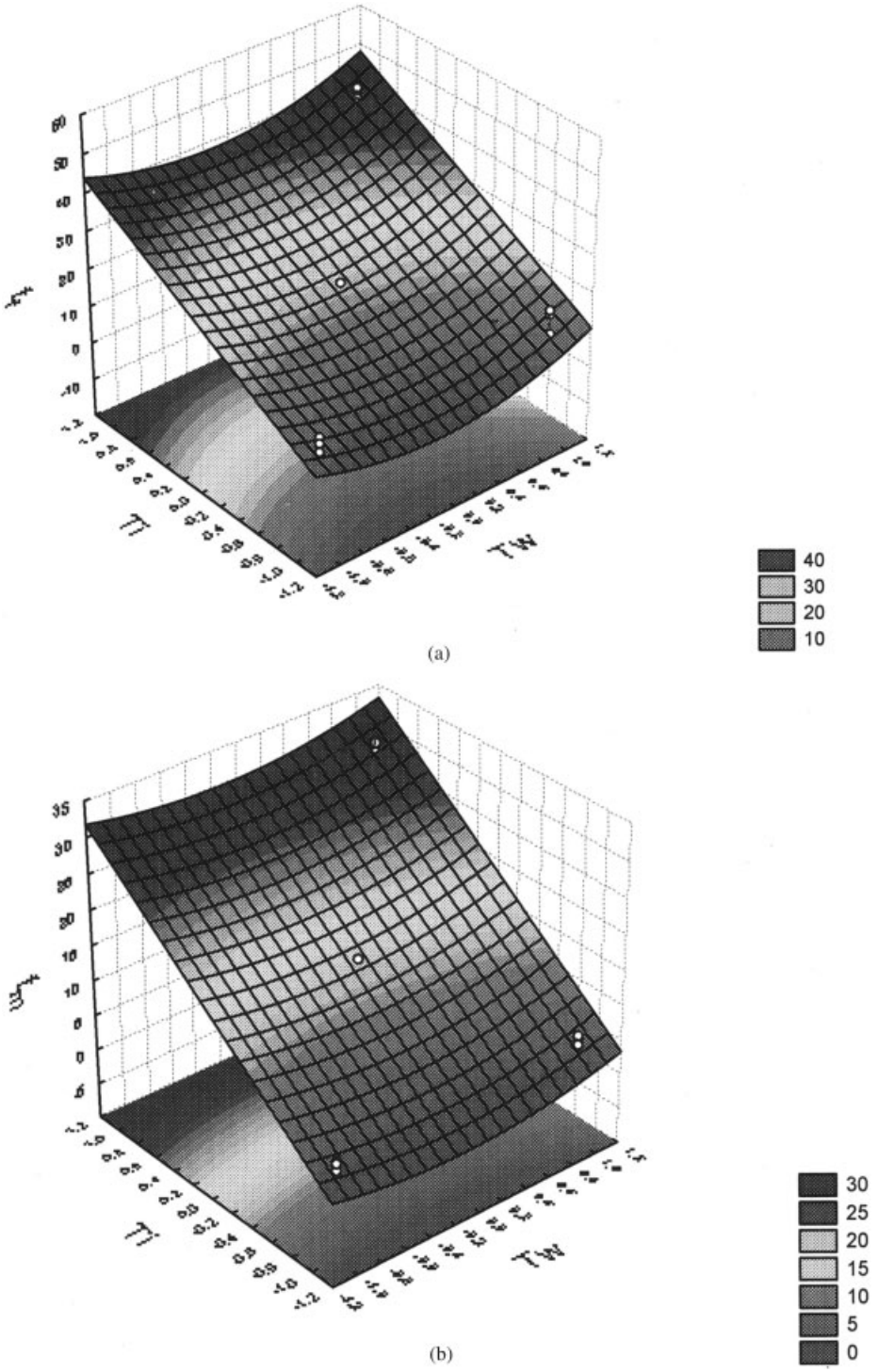

Figure 15 Response surfaces showing the influence of T_i and T_w on: (a) t_f of PTT; (b) t_m of PTT.

Comparing the backscattering behavior of the PP, PBT, and PTT, it can be concluded that probably the backscattering absence in PP was due to its crystal density (0.905 g/cm^3), lower than that of both polyesters (ρ_{PBT} = 1.31 g/cm^3, ρ_{PTT} = 1.35 g/cm^3).

It can be observed that the PBT crystallization is much faster than the PTT; that as the crystallization proceeds, the pressure decreases, as expected; and that the packing pressure seems to influence the backscattering behavior of the PTT but not of the PBT.

The distinctive minimum in the intensity data at t $\cong$ 5s for the PBT sample, and at t $\cong$ 35s for the PTT sample, is attributed to light scattering by polymer spherulites, which was first observed by Stein and coworkers.[13,14] This distinctive minimum is a universal observation, present in all curves,[1,15,16] and it cor-

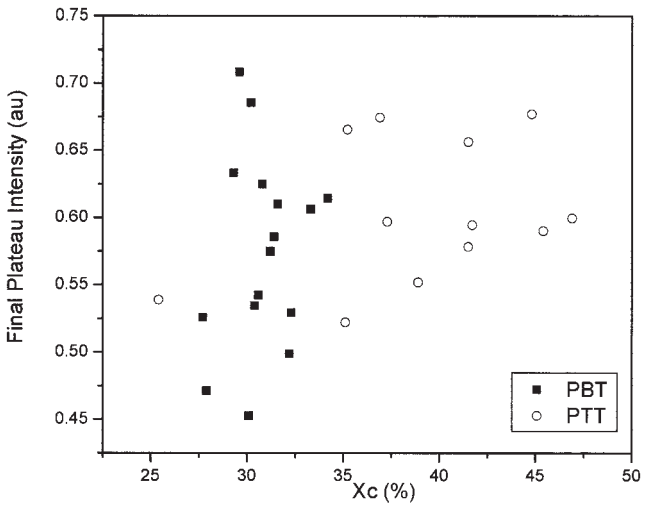

Figure 16 Correlation between the final plateau of the light intensity signal curves and the amount of crystallinity.

responds to the time when most of the material crystallizes in the spherulitic form, essentially at the central core. From this moment on, the crystal volume fraction becomes higher than the amorphous volume fraction, and therefore the light scattering is low, due to the decrease of the amount of amorphous/crystalline interfaces. So, a continuous increase of the signal is observed until it reaches a final plateau.[1,15,32] This final plateau, which occurs just after the characteristic minimum, is associated with the end of crystallization.

The PET curves, as can be seen in Figure 9, had a completely different behavior at all processing conditions. The majority of the signals decreased with time, attaining a plateau almost instantaneously.

Due to this complex behavior, it was decided to choose three different characteristic times, which are also shown in Figure 8:

a. t_i = time at which crystallization began (right after the filling stage 2);
b. t_m = time at which the backscattering contribution was the strongest one (the minimum in the light intensity signal related to polymer critical crystal size);
c. t_f = time at which crystallization ends.

The choice of the time t_i as the beginning of the crystallization was based on the assumption that right after touching the mold walls, the polymer melt will begin to crystallize. The t_i time was considered the zero of all curves.

Figures 10 and 11 show the curves obtained for the injection molding of the PBT and PTT, respectively, while Tables III and IV show the crystallization characteristic times of both polymers. For the PET, t_m and t_f were not observed. Comparing the results from the different processing conditions, it can be observed that, as a general rule:

1. The light intensity signal varies with the flow rate, showing that the crystallization occurs early when the flow rate increases.
2. When the mold temperature is increased, the positions of the characteristic times for the

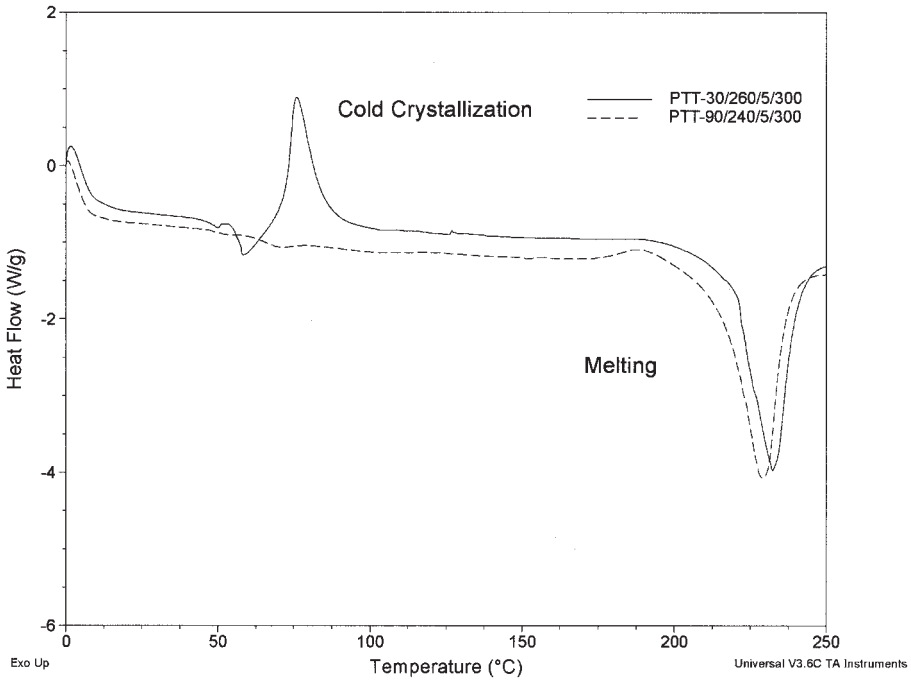

Figure 17 Standard DSC curves for the PTT injection molded samples.

same flow rate and packing pressure conditions are shifted to higher values, that is, the crystallization is retarded.
3. When the injection melting temperature is increased, the characteristic times are also shifted to higher values.
4. The interpretation of the signals is quite difficult when the material develops low crystallinity, as in the case of the PET.

It can also be noted that an abrupt increase of the signal occurred at the ending of the crystallization process for some of the samples injected at low holding pressures. This abrupt increase can be a consequence of the separation of the solidified polymer from the mold wall.

Figures (12–14) show typical morphologies of the PBT, PTT, and PET samples, respectively, observed by PLOM; while Table V shows the overall crystallinity degree, X_c, of the polyesters, evaluated by DSC. As observed from the optical signals, the PET samples developed very little or no crystallinity at all. Regarding the morphology, it can be observed that at low mold temperatures, PBT and PTT had an amorphous layer. This amorphous layer disappeared when the mold temperature was raised to 90°C. At low injection temperatures, the samples showed a dark nucleus, which can be a consequence of a stronger nucleation process or a high molecular orientation at this region. The relationships between the optical signals and the morphology will be further investigated.

To identify the variables that affected more the crystallization process during the injection molding and the interactions between those variables, a variance analysis was made on the experimental data, as already explained. As said before, a statistical significance, or *p*-level, equal to 0.05 was chosen to identify the reliability of the main effects of the variables and interactions between them. However, values of the *p*-level higher than 0.05 were also accepted.

Tables VI and VII show the coefficients of the second order polynomials [eq. (3)] that had statistical significance, for each one of the characteristic times of the PBT and PTT crystallization, respectively. The variations around the average given by the regression models, R^2, are also shown.

For the PBT, regarding t_m, the main effect was only given by T_w, and it was positive, that is, increasing T_w increases t_m. Interactions between the effects were also observed, which indicate that the influence of T_w will depend on the Q and P values. Regarding t_f, the main effects were given by T_w and T_i, and were also positive. However, the T_w influence will depend on the P value.

For the PTT, regarding t_m, positive main effects were given by T_w and T_i; negative effect was given by Q, that is increasing Q, decreases t_m. No interactions between these effects were observed. Regarding t_f the same behavior as with t_m was observed; however, interactions between T_w, T_i, and Q were observed. No influence of the holding pressure was observed.

The influence of T_w and T_i on the crystallization process of the PTT injection molding can also be analyzed by the response surfaces shown in Figure 15. Its crystallization occurred earlier (both t_f and t_m are lower) when T_w increased until approximately 60°C. However, after this value, both crystallization times again increase. The linear increase of t_f and t_m with T_i can also be observed from these response surfaces.

Finally, in Figure 16, the overall degree of crystallinity (evaluated by DSC) is plotted versus the light intensity of the final plateau for all the PBT and PTT samples. Typical DSC traces can be observed in Figure 17 for the PTT injection molded samples, from which the overall degree of crystallinity was evaluated from eq. (4). It is known that the opacity of a sample can be related to its global crystallinity. Therefore, it would be expected that the higher the X_c, the higher the opacity of the sample, which means the lower should be the light intensity final plateau. A linear inverse relationship was found by Thomas and Bur for PP.[1,32] However, from Figure 16, it can be seen that the final plateau intensity of the polyesters was not a function of the bulk crystallinity of the samples, probably due to the strong backscattering observed in these polymers.

CONCLUSIONS

The optical device built in this work was shown to be a reliable one. The light intensity signal was reproducible and extremely sensitive to changes in the injection molding processing conditions. The measurements showed that this system was sensitive to variations of the crystallization of different kinds of polymers under different processing conditions. The system was not able to monitor, however, the crystallization process when the crystallinity degree developed by the sample was very low, as in the PET resin. It was also observed that T_w and T_i were the most influential variables on the crystallization kinetics of PBT and PTT. Due to its slower crystallization kinetics, PTT was found to be more sensitive to changes of the molding variables than PBT. It was found that the final plateau intensity has no correlation to the bulk crystallinity of the samples, probably due to the strong backscattering observed in the polyesters.

The authors thank FAPESP and PRONEX for financial aid; Rhodia-Ster, GE Plastics South America, and Shell Chemicals for the donation of the samples; and Dr. Anthony J. Bur and Dr. J. Magill for their kindness on answering our requests.

References

1. Thomas, C. L.; Bur, A. J. Polym Eng Sci 1999, 39, 1291.
2. Zheng, R.; Kennedy, P. Modeling Flow-Induced Crystallization; 19th Annu Meeting of the Polym Proc Soc., Melbourne, Australia, July 7–10, 2003.
3. Kennedy, P.; Zheng, R. Prediction of Flow-Induced Crystallization in Injection Molding; 19th Annu Meeting of the Polym Proc Soc., Melbourne, Australia, July 7–10, 2003.
4. Kennedy, P.; Zheng, R. Crystallization and Simulation of Injection Molding, September 19–20, 2003, Polymer Crystallization and Structure Formation in Processing Meeting—20 Years of Fundamental and Applied Research in Linz, Johannes Kepler University *PC2003*, Univ Linz.
5. Guillet, J.; Gonnet, J. M.; Sirakov, I.; Fulchiron, R.; Seytre, G. On-Line Monitoring of the Injection Molding Process by Dielectric Spectroscopy; 17th Annu Meeting of the Polym Proc Soc, Montreal, Canada, May 21–24, 2001.
6. Wang, H.; Cao, B.; Jen, C. K.; Nguyen, K. T.; Viens, M. Polym Eng Sci 1997, 37, 363.
7. Brown, E. C.; Dawson, A. J.; Coates, P. D. Ultrasonic Measurements in the Nozzle and Cavity during Injection Molding; 17th Annu Meeting of the Polym Proc Soc, Montreal, Canada, May 21–24, 2001.
8. La Carruba, V.; Gabriëlse, W.; Van Gurp, M.; Picarollo, S.; Brucato, V.; Optimization of Cycle time in Injection Molding through the study of solidification by an Indentation Test, September 19–20, 2003, Polymer Crystallization and Structure Formation in Processing Meeting—20 Years of Fundamental and Applied Research in Linz, Johannes Kepler University *PC2003*, Univ Linz.
9. Magill, J. H. Polymer 1961, 2, 221.
10. Magill, J. H. Polymer 1961, 3, 35.
11. Magill, J. H. Nature 1960, 187, 770.
12. Birnboim, M. H.; Magill, J. H.; Berry, G. C. A Microbeam Light Scattering Technique for Studying Spherulite Morphology; 2nd Int Conf on Eletromagnetic Scattering, Univ. of Massachusetts, June 1965.
13. Rhodes, M. B.; Stein, R. S. J Polym Sci 1960, 45, 521.
14. Yoon, D.Y.; Stein, R. S. J Polym Sci Polym Phys 1974, 12, 735.
15. Ding, Z.; Spruiell, J. E. J Polym Sci Part B 1996, 34, 2783.
16. Lamberti, G.; de Santis, F.; Brucato, V.; Tittomanlio, G. Appl Phys A: Mat Sci Proc 2004, 78, 895.
17. Chrishman, R. W.; McLachlan, R. D.; Harner, R. S. U.S. Patent 4,672,218, 1987.
18. Farah, M.; Bretas, R. E. S. Caracterização Reológica de Poliésteres de Engenharia para Moldagem por Injeção; 6º Congresso Brasileiro de Polímeros, Gramado, Brasil, CBPOL, ABPol, Nov 11–15, 2001.
19. Billmeyer Jr., F. W. Textbook of Polymer Science; John Wiley & Sons Inc: New York, 1984.
20. Rao, M. V. R. M.; Yassen, M. J Appl Polym Sci 1986, 31, 2501.
21. Chee, K. K. J Appl Polym Sci 1987, 34, 891.
22. Chuah, H. H.; Lin-Vien, D.; Soni, U. Polymer 2001, 42, 7137.
23. Randrup, J.; Immergut, E. H.; Grulke, E. A. Polymer Handbook; John Wiley and Sons, Inc: New York, 1999.
24. Orman, W. F. H. J Appl Polym Sci 1978, 22, 2119.
25. Lotti, C.; Ueki, M. M.; Bretas, R. E. S. J Inj Mold Tech 2002, 6, 157.
26. Barros Neto, B.; Scarminio, I. S.; Bruns, R. E. Planejamento e Otimização de Experimentos; EdUnicamp: São Paulo, Brazil, 1995.
27. Antony, J. Microeletronics J 1999, 30, 161.
28. Coit, D. W.; Jackson, B. T.; Smith, A. E. Int J Prod Res 1998, 36, 2953.
29. Fakirov, S.; Aavramova, N.; Schultz, J. Die Angewandte Makromoleculare Chemie 1986, 140, 63.
30. Chuah, H. H. Polym Eng Sci 2001, 41, 308.
31. Yao, N. Polymer 1993, 34, 1564.
32. Bur, A. J.; Thomas, C. L. U.S. Patent 5,519,211, 1996.
33. Lamberti, G.; de Santis, F.; Giannattasio, A.; Brucato, V.; Titomanlio, G. An Experimental Set-Up for Real Time Measurements of Non-Isothermal Crystallization Kinetics; 18th Annu Meeting of the Polym Proc Soc, Guimaraẽs, Portugal, June 18–21, 2002.